


 Cite this: *Chem. Commun.*, 2022, 58, 7427

 Received 19th April 2022,  
 Accepted 8th June 2022

DOI: 10.1039/d2cc02236b

rsc.li/chemcomm

# Mixed-metal calix[8]arene complexes: structure, and ring opening polymerisation studies†

 Tian Xing,<sup>a</sup> Max Derbyshire,<sup>b</sup> Mark R. J. Elsegood <sup>b</sup> and Carl Redshaw <sup>\*a</sup>

**Reactions of different combinations of group V alkoxides or tungsten oxyalkoxide salts with *p*-tert-butylcalix[8]areneH<sub>8</sub> (L<sup>8</sup>H<sub>8</sub>) affords mixed-metal calix[8]arene systems. Intriguing molecular structures are formed and the systems are capable of the ring opening polymerisation of  $\epsilon$ -caprolactone under N<sub>2</sub>, air, or as melts affording mostly low molecular weight products.**

The use of calix[*n*]arenes as ancillary ligands in metal-based catalysis continues to attract interest, driven in part by the facile functionalisation of calixarenes as well as the tendency of such systems to form highly crystalline products.<sup>1</sup> In the case of the larger calix[*n*]arenes (*n* ≥ 6), there is the increased possibility of simultaneously coordinating multiple metal centres.<sup>2</sup> Over the last decade or so, a number of metallocalix[*n*]arenes have been shown to be useful catalysts for the ring opening polymerisation (ROP) of cyclic esters.<sup>3</sup> Such a ROP process has become topical given the need to find alternatives to petroleum-derived plastics.<sup>4</sup> In ROP, the use of heterometallic catalysts is an emerging area,<sup>5</sup> whilst the use of polymetallic systems has also been deemed favourable.<sup>6</sup> The driving force in such studies is the possibility that cooperativity between metal centres can lead to enhanced catalytic performance *versus* homometallic or mono-metallic counterparts.<sup>7</sup> In our previous work, we have reported vanadium-containing calixarenes, and have been able to structurally characterise examples containing one, two, three, or four vanadyl centres bound to a calix[8]arene.<sup>8</sup> Our entry into such systems is typically *via* the use of alkoxides of the form [V(O)(OR)<sub>3</sub>] (*R* = Et, *n*Pr), which react with the parent calixarene with loss of alcohol (ROH). Herein, we have extended our investigations to the synthesis of mixed-metal calix[8]arene

systems, containing either different group V metals or combinations of group V and VI metals, formed *via* the use of alkoxide precursors. The potential of such systems to act as catalysts for the ROP of  $\epsilon$ -caprolactone has been investigated. We note that mixed-metal calixarene complexes are limited to Fe<sub>2</sub>Ln<sub>2</sub> *p*-tert-butylcalix[4]arene clusters (Ln = lanthanide)<sup>9a</sup> and Mn<sub>4</sub> (M = Mn, Co, Cu) *p*-tert-butylthiacalix[6]arene clusters.<sup>9b</sup>

Our entry point into this chemistry are the commercially available reagents [M(OEt)<sub>5</sub>] (M = Nb, Ta), [VO(OR)<sub>3</sub>] (*R* = *i*Pr, *n*Pr), [MoO(O*i*Pr)<sub>4</sub>] and the *in situ* generated Li[WO(O*t*Bu)<sub>5</sub>]. Treatment of L<sup>8</sup>H<sub>8</sub> with one equivalent each of [VO(*Oi*Pr)<sub>3</sub>] and [Nb(OEt)<sub>5</sub>] afforded, following work-up, the complex [{Nb(*Oi*Pr)(NCMe)}<sub>2</sub>( $\mu$ -O)<sub>3</sub>(VO)<sub>2</sub>(L<sup>8</sup>)]·8MeCN (**1-8MeCN**) in moderate yield; the molecular structure of **1-8MeCN** is shown in Fig. 1 (for packing see Fig. S1, ESI†). In the IR spectrum,  $\nu$ (CN) for the coordinated/free acetonitrile are observed at 2289/2251 cm<sup>-1</sup>, whilst the strong band at 1013 cm<sup>-1</sup> is assigned to  $\nu$ V=O; bands in the region 800–600 cm<sup>-1</sup> are assigned to  $\nu$ Nb–O–Nb and  $\nu$ Nb–O–V. The formula given is the asymmetric unit. The two

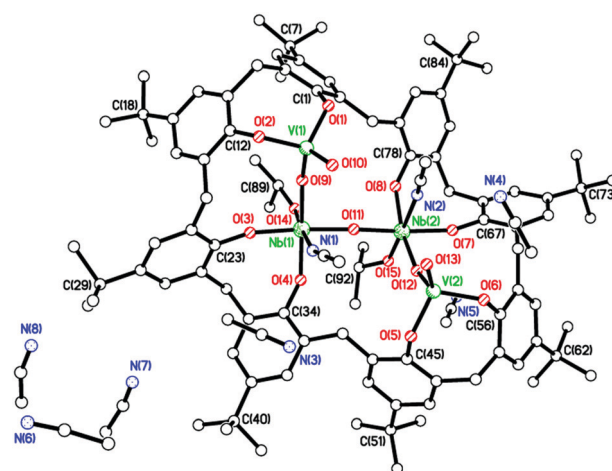


Fig. 1 Molecular structure of [{Nb(*Oi*Pr)(NCMe)}<sub>2</sub>( $\mu$ -O)<sub>3</sub>(VO)<sub>2</sub>(L<sup>8</sup>)]·8MeCN (**1-8MeCN**).

<sup>a</sup> *Plastics Collaboratory, Department of Chemistry, University of Hull, Cottingham Road, Hull, HU6 7RX, UK. E-mail: c.redshaw@hull.ac.uk*

<sup>b</sup> *Chemistry Department, Loughborough University, Loughborough, Leicestershire, LE11 3TU, UK*

† Electronic supplementary information (ESI) available: Synthetic details for **1-7**; alternative views of **1-7**; crystallographic and ROP data. CCDC 2156668–2156674. For ESI and crystallographic data in CIF or other electronic format see DOI: <https://doi.org/10.1039/d2cc02236b>



octahedral niobium(v) centres are bridged by a near symmetric, slightly bent [Nb(1)–O(11)–Nb(2) = 162.73(14)°] oxo bridge. Each niobium centre is bound by an isopropoxide ligand, an MeCN and *cis* bonds to two calixarene phenolate oxygens, whilst the two tetrahedral vanadium centres bridge to one Nb each *via* an oxo bridging ligand. Each V<sup>5+</sup> has a second, terminal, oxo ligand, and this vanadyl bond length at 1.603(2) Å is in the range [1.593(2)–1.695(4) Å] typically observed for this function.<sup>8</sup> The two VO<sub>2</sub><sup>+</sup> moieties are both ‘above’ the Nb–O–Nb unit in the heart of the complex.

This type of structural motif seems quite general, given that similar use of [Ta(OEt)<sub>5</sub>] also led to an isostructural complex, namely {[Ta(OiPr)(NCMe)]<sub>2</sub>(μ-O)<sub>3</sub>(VO)<sub>2</sub>(L<sup>8</sup>)}·6.5MeCN (2·6.5MeCN), differing only in the number of MeCNs of crystallisation (Fig. S2, ESI<sup>†</sup>). In the IR spectrum of 2·6.5MeCN, a band at 1012 cm<sup>−1</sup> is assigned to νV=O.

Surprisingly, replacing [VO(OiPr)<sub>3</sub>] with [VO(OnPr)<sub>3</sub>] led, following work-up, to the isolation of the complex [Nb<sub>2</sub>(VO)<sub>2</sub>{VO(OnPr)}{V(NCMe)<sub>2</sub>}(μ<sub>2</sub>-OnPr)<sub>2</sub>(μ<sub>3</sub>-O)(μ<sub>2</sub>-O)<sub>2</sub>(L<sup>8</sup>)]·7MeCN (3·7MeCN), see Fig. 2 and Fig. S3 (ESI<sup>†</sup>). In the IR spectrum, the strong band at 1021 cm<sup>−1</sup> is assigned to νV=O. Whilst the metal centres V(1) and V(2) do not coordinate to the calix[8]arene, the other four metal centres each coordinate to two adjacent calix[8]arene phenolates. The V(1) centre adopts a distorted octahedral geometry where the coordination sphere is completed by two acetonitrile ligands. The V(2) centre is distorted trigonal bipyramidal, as confirmed by the Reedijk criteria (τ = 0.06),<sup>10</sup> and is bound by all three of the *n*-propoxide ligands; two of the latter form bridges to the two octahedral niobium centres. It is noteworthy that whilst three of the vanadium centres are of the vanadyl [V=O] type, V(3) is not.

The vanadyl bond lengths [1.566(3)–1.588(3) Å] are comparable with those observed in 1·8MeCN [1.589(3) and 1.603(2) Å] and 2 [1.583(8) and 1.603(7) Å]. The geometry at both V(3) and V(4) is tetrahedral, with each metal lying above/below the

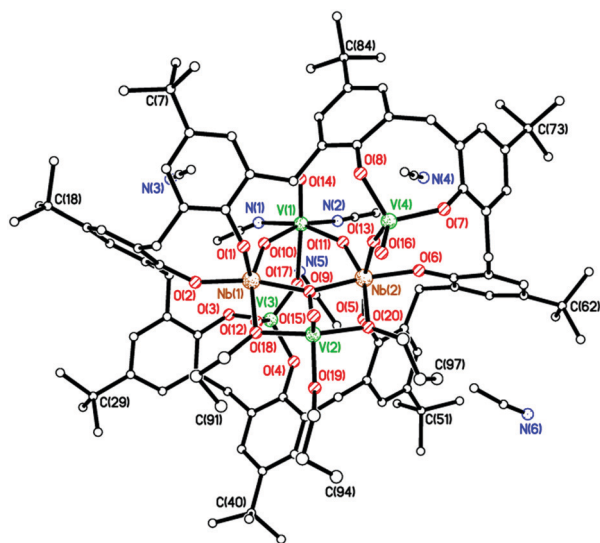


Fig. 2 Molecular structure of [Nb<sub>2</sub>(VO)<sub>2</sub>{VO(OnPr)}{V(NCMe)<sub>2</sub>}(μ<sub>2</sub>-OnPr)<sub>2</sub>(μ<sub>3</sub>-O)(μ<sub>2</sub>-O)<sub>2</sub>(L<sup>8</sup>)]·7MeCN (3·7MeCN).

approximate plane formed by the other four metal centres. Within the core, a 6-membered triangle is formed involving Nb(1), Nb(2), V(1) and three oxo bridges. A second triangle is formed by V(1), V(3), Nb(1) and three μ<sub>2</sub>-oxo bridges. Moreover, two diamond motifs are generated by the ligation between V(2), two bridging *n*-propoxides, a μ<sub>3</sub>-oxo and the niobium centres. Platon suggests that the V(1) centre is the 4+ centre.<sup>11</sup>

In an attempt to extend this chemistry to mixed group V/VI systems, [M(OR)<sub>5</sub>] (M = Nb, Ta) was reacted with L<sup>8</sup>H<sub>8</sub> in the presence of [WO(OtBu)<sub>4</sub>]. However, the crystals isolated consistently suffered from severe disorder making structure elucidation problematic. Given this, it was decided to employ a salt complex of the form Li[WO(OtBu)<sub>5</sub>] as the entry point, which was generated *in situ* *via* interaction of [WO(OtBu)<sub>4</sub>] with LiOtBu, akin to the method of Wilkinson *et al.*<sup>12</sup> for other metal salts.

Interaction of Li[WO(OtBu)<sub>5</sub>], [Nb(OR)<sub>5</sub>], and L<sup>8</sup>H<sub>8</sub> led, after work-up (MeCN), to the isolation of orange/red crystals of [{WO(NCMe)<sub>2</sub>(μ<sub>2</sub>-O)<sub>2</sub>Nb(NCMe)(μ<sub>2</sub>-O)Li(NCMe)(L<sup>8</sup>)]·4MeCN (4·4MeCN), see Fig. 3 and Fig. S4 (ESI<sup>†</sup>). In the IR spectrum, a band at 915 cm<sup>−1</sup> is assigned to νW=O, whilst bands at 2318/2294 cm<sup>−1</sup> are assigned to the metal-bound acetonitrile ligands. The two octahedral W(vi) centres have three (*mer*) bonds, a terminal oxo group, a near linear oxo bridge (to Nb) and an acetonitrile ligand. The W=O bond lengths [1.691(4) and 1.710(3) Å] are in good agreement with others observed in tungstocalixarenes.<sup>13</sup> The Nb(v) centre is also octahedral but with two *cis* bonds to the calixarene, three *fac* bonds to bridging oxo groups (two to W, one to Li) and an acetonitrile ligand. The Nb–N bond lengths [2.416(4) and 2.449(4) Å] are slightly longer than those observed in a number of reported niobium aryloxide acetonitrile species [2.220(13)–2.321(2) Å].<sup>14</sup> The tetrahedral Li centre bonds to two calixarene oxygens, the oxo bridge to niobium, and an acetonitrile ligand.

Given the presence of oxo bridges in 4·4MeCN, the reaction was repeated using L<sup>8</sup>H<sub>8</sub> that had been subject to prolonged

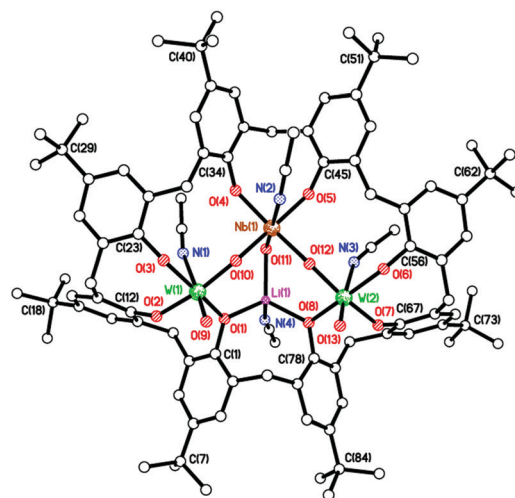


Fig. 3 Molecular structure of one of two similar molecules in the asymmetric unit of [{WO(NCMe)<sub>2</sub>(μ<sub>2</sub>-O)<sub>2</sub>Nb(NCMe)(μ<sub>2</sub>-O)Li(NCMe)(L<sup>8</sup>)]·4MeCN (4·4MeCN); solvent of crystallization omitted for clarity.



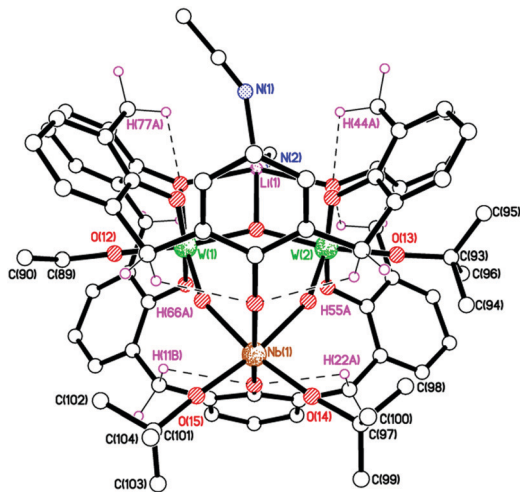


Fig. 4 Molecular structure of  $[\text{Li}(\text{NCMe})_2\{\text{WO}(\text{O}t\text{Bu})\}\{\text{WO}(\text{OEt})_a(\text{O}t\text{Bu})_b\}\{\text{NbO}(\text{OEt})_c(\text{O}t\text{Bu})_d\}\text{L}^8]\cdot 3\text{MeCN}$  (5·3MeCN); solvent of crystallization omitted for clarity.

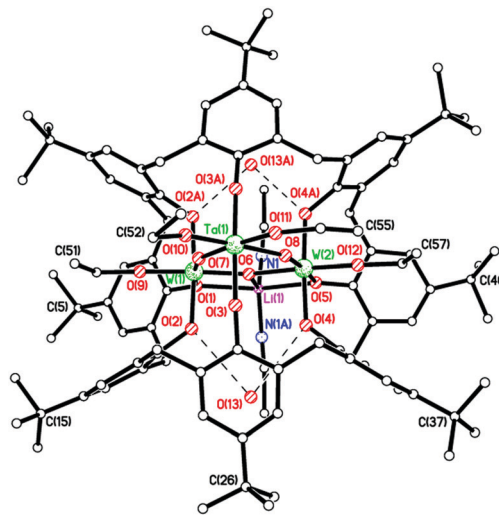


Fig. 5 Molecular structure of  $[\text{Li}(\text{NCMe})_2\{\text{W}(\text{OEt})_2\text{Ta}(\text{OEt})_2\text{O}_3\text{L}^8\}\cdot 2(\text{H}_2\text{O})$  (6·2H<sub>2</sub>O).

drying (48 h at 100 °C under *vacuo*). Following work-up (MeCN), small red prisms were isolated. In the IR spectrum, a band at 921 cm<sup>-1</sup> is assigned to  $\nu\text{W}=\text{O}$ , whilst bands in the region 820–600 cm<sup>-1</sup> are assigned to  $\nu\text{W}-\text{O}-\text{W}$  and  $\nu\text{Nb}-\text{O}-\text{W}$ . A single crystal X-ray diffraction study revealed the product to be  $[\text{Li}(\text{NCMe})_2\{\text{WO}(\text{O}t\text{Bu})\}\{\text{WO}(\text{OEt})_a(\text{O}t\text{Bu})_b\}\{\text{NbO}(\text{OEt})_c(\text{O}t\text{Bu})_d\}\text{L}^8]\cdot 3(\text{MeCN})$  (5·3MeCN), Fig. 4 and Fig. S5 (ESI<sup>†</sup>). Again, the presence of two octahedral W(vi) centres and a Nb(v) centre is clear and these are bridged by three oxo ions O(9), O(10), and O(11). The oxygen bridging the two tungsten centres is also coordinated to a lithium centre. The W=O bond lengths 1.775(3) and 1.765(3) Å are slightly longer than those observed in 4·4MeCN, but are still in good agreement with others observed elsewhere.<sup>13</sup> Interestingly, the structure is stabilised *via* eight weak hydrogen bonding interactions between CH<sub>2</sub> groups of the calix[8]arene ligand and respective metal coordinative phenolate oxygen atoms, see ESI<sup>†</sup>. The three transition metals form a triangle, and the lithium ion is in the same plane, whilst the calix[8]arene adopts a saddleback conformation; alkoxide ligands are in the two main cavities.

Interaction of  $\text{Li}[\text{WO}(\text{O}t\text{Bu})_5]$ ,  $[\text{Ta}(\text{OEt})_5]$  and  $\text{L}^8\text{H}_8$  led, after work-up (MeCN), to the isolation of small orange/red crystals of  $[\text{Li}(\text{NCMe})_2\{\text{W}(\text{OEt})_2\text{Ta}(\text{OEt})_2\text{O}_3\text{L}^8\}\cdot 2(\text{H}_2\text{O})$  6·2H<sub>2</sub>O, see Fig. 5 and Fig. S6 (ESI<sup>†</sup>). It should be noted here that given W(vi) and Ta(v) have the same number of electrons, their positions in the formula are interchangeable. Despite this, the metal centres in the core form the type of triangle noted in 3·7MeCN with oxo bridges. In the same plane (a crystallographic mirror plane), there is a 5-coordinate Li<sup>+</sup> ion. The two (symmetry equivalent) metal (W or Ta) centres are octahedral and coordinate to two oxo anions, three calixarene phenolate oxygens and an ethoxide. The Ta (or W) ion binds to two *cis* ethoxides, two *trans* calixarene phenolates and two *cis* oxo anions. The oxo ions O(7)/O(8) make long bonds to the Ta at *ca.* 2.12 Å (*trans* to ethoxide), but much shorter bonds to the two W ions at *ca.* 1.75 Å (*trans* to calixarene phenolate).

Attempts to form a mixed tantalum (or niobium)-molybdenum complex *via*  $[\text{M}(\text{OEt})_5]$  (M = Nb, Ta),  $[\text{MoO}(\text{O}i\text{Pr})_4]$ <sup>15</sup> and  $\text{L}^8\text{H}_8$  led, after work-up, to the dimetallic complex  $[\{\{\text{MoO}(\text{NCMe})\}\}_2\text{L}^8]\cdot 5\text{MeCN}$  (7·5MeCN) as the only crystalline product in low isolated yield, see Fig. S7, ESI<sup>†</sup>.

Complexes 1,2,5,6 have been screened for their potential to act catalysts for the ROP of  $\epsilon$ -caprolactone. Despite the presence of alkoxide ligation in most of these precursors, we found that addition of benzyl alcohol (BnOH) can still be beneficial in terms of overall performance. Using 1, the ratio [CL]:[1]:[BnOH], time and temperature were all varied, see Table S2, ESI<sup>†</sup>. At ambient temperature, in the presence of two equivalents of BnOH, and using a ratio of 800:1 ([CL]:[1]), the conversion was high over 24 h, but the products formed were of low molecular weight. Increasing the temperature to 100 °C led to an increased molecular weight, which further increased on raising the temperature to 130 °C, but led to a less controlled process. In the absence of BnOH, the performance of the system was similar. Complex 2 performed less well at 20 °C with only 30% conversion, whilst on raising the temperature to 130 °C, the conversion was near quantitative affording a product of lower molecular weight than 1 but with better control. In the absence of BnOH, high conversion is maintained whilst the PCL molecular weight is higher. For 3, conversions are high, with higher molecular weight observed in the presence of BnOH. The tungsten/niobium/lithium complex 5 affords only low molecular weight products at ambient temperature, with or without BnOH present. At 130 °C, the molecular weight is increased significantly only in the absence of BnOH. Similarly, the tungsten/tantalum/lithium complex 6 afforded only low molecular weight PCL at room temperature, whilst on elevating the temperature, there was little change. Kinetic studies (Fig. S8i, ESI<sup>†</sup>), conducted using 800:1:2 ([CL]:[Cat]:[BnOH]) revealed the rate trend 6 > 2 > 5 > 1. For comparative purposes, the homo-dinuclear complexes  $[\{\text{MCl}_2\text{L}^8\text{H}_2\}]$  (M = Nb I, Ta II) have also been screened herein under similar conditions.<sup>14b</sup> Results reveal that, as for the mixed-metal systems 1, the Nb system I



exhibits higher conversion at ambient temperature than does Ta system **II**, with all affording low molecular weight products ( $M_n \leq 910$ ). At 130 °C, the Ta system afforded higher conversion, however the  $M_n$  value observed for **II** was twice that for **I**, whereas that obtained using **1** was three times greater than that for **2**, albeit with worse control. On comparing **I** with **1** at 130 °C, it can be said that better conversion is achieved with the mixed-metal system and a higher molecular product afforded, but with less control. For **2**, conversion is slightly greater than **II**, whilst the latter affords a higher molecular weight product, but with less control.

$^1\text{H}$  NMR spectra of PCL formed in the presence of BnOH indicated the presence of a BnO end group (e.g. Fig. S9, ESI $^\dagger$ ). However, from MALDI-ToF mass spectra (Fig. S10 and S11, ESI $^\dagger$ ), it was evident that several PCL series were present (as sodium adducts). For **1**, these included (in increasing mass order) a series with BnO-/-H (with  $n - 1$  degree of polymerisation), a series with no end groups (cyclic), HO-/-H (and a -2Da offset series overlapping),  $\text{CH}_3\text{O-/-H}$  and  $\text{iPrO-/-H}$ . Similarly, for **2**, four PCL series can be identified which include a series with no end groups, HO-/-H and the sodium exchange artefact, and BnO-/-H end groups. Some of these families were evident in  $^1\text{H}$  NMR spectra for runs in the absence of BnOH (e.g. Fig. S12, ESI $^\dagger$ ).

Interestingly, in the absence of BnOH, kinetics revealed (Fig. S8ii, ESI $^\dagger$ ) the activity order  $5 \gg 1 \approx 6 \approx 2$  with the Nb/W/Li system outperforming the other three under the conditions employed herein. The reason for this differing trend is as yet unknown, but we tentatively suggest that the presence of the *tert*-butoxide is beneficial. The complexes were examined for their ROP potential under solvent-free conditions (Table S3, ESI $^\dagger$ ). Results for **1** were similar with or without BnOH, whilst for **2**, use of BnOH led to a higher molecular weight product albeit with less control. The performance of **5** was poor in the presence of BnOH, but improved in the absence of BnOH with a 10-fold increase in conversion and an approximate 4-fold increase in product molecular weight. The situation using **6** was somewhat different with a slightly improved conversion in the presence of BnOH, together with an increased molecular weight. Again,  $^1\text{H}$  NMR spectra of the PCL formed in the presence of BnOH indicated the presence of a BnO end group (Fig. S13, ESI $^\dagger$ ).

Finally, the complexes were evaluated for ROP of  $\epsilon\text{-CL}$  under air (Table S4, ESI $^\dagger$ ). In general, higher conversions were achieved in the absence of BnOH, with **1** affording highest conversion. With the exception of **1**, molecular weights of the products obtained under air, in the presence of BnOH, were comparable with those afforded under  $\text{N}_2$ ; that for **1** was somewhat lower. In the absence of BnOH, molecular weights were generally higher than those observed under  $\text{N}_2$ . The MALDI-ToF mass spectra (Fig. S14–S16, ESI $^\dagger$ ), for **1**, show a low mass series with no end groups (not shown), plus a series with HO-/-H and the sodium exchange artefact where the carboxylic proton has exchanged for Na. For **2**, at least four series of peaks were identified including the sodium exchange

artefact for the BnO-/-H end group (e.g.  $m/z$  1407.8), overlapping (-2 Da offset) with the HO-/-H series, together with a number of lower intensity families. In the absence of BnOH, **2** affords similar species to that formed with BnOH except for the BnO-/-H series. There is also a +4Da offset from the no end group series (e.g.  $m/z$  1395.8).

In conclusion, we have isolated and structurally characterised a number of rare examples of mixed-metal calix[ $n$ ]arenes using group V and VI alkoxides as entry points. A number of unusual structures have been identified. The products are capable of the efficient ROP of  $\epsilon\text{-CL}$ , affording mixtures of low molecular weight products with differing or no end groups.

We thank the China Scholarship Council (CSC) for a PhD Scholarship with TX. CR thanks the EPSRC (EP/S025537/1) for financial support. We thank the EPSRC National Crystallography Service, Southampton for data collection and Wyatt Analytical for data.

## Conflicts of interest

There are no conflicts to declare.

## References

- (a) D. H. Homden and C. Redshaw, *Chem. Rev.*, 2008, **108**, 5086–5130; (b) O. Santoro and C. Redshaw, *Coord. Chem. Rev.*, 2021, **448**, 214173.
- C. Redshaw, *Coord. Chem. Rev.*, 2003, **244**, 45–70.
- (a) M. Frediani, D. Sémeril, A. Marriotti, L. Rosi, P. Frediani, L. Rosi, D. Matt and L. Toupet, *Macromol. Rapid Commun.*, 2008, **29**, 1554–1560; (b) M. Frediani, D. Sémeril, D. Matt, L. Rosi, P. Frediani, F. Rizzolo and A. M. Papini, *Int. J. Polym. Sci.*, 2010, **490724**, 6.
- For reviews, see (a) B. J. O'Keefe, M. A. Hillmeyer and W. B. Tolman, *J. Chem. Soc., Dalton Trans.*, 2001, 2215–2224; (b) O. Dechy-Cabaret, B. Martin-Vaca and D. Bourissou, *Chem. Rev.*, 2004, **104**, 6147–6176; (c) M. Labet and W. Thielemans, *Chem. Soc. Rev.*, 2009, **38**, 3484–3504; (d) C. M. Thomas, *Chem. Soc. Rev.*, 2010, **39**, 165–173; (e) A. Arbaoui and C. Redshaw, *Polym. Chem.*, 2010, **1**, 801–826; (f) Y. Sarazin and J.-F. Carpentier, *Chem. Rev.*, 2015, **115**, 3564–3614 and references therein.
- W. Gruszka and J. A. Garden, *Nat. Commun.*, 2021, **12**, 3252.
- (a) J. D. Ryan, K. J. Gagnon, S. J. Teat and R. D. McIntosh, *Chem. Commun.*, 2016, **52**, 9071–9073; (b) E. Fazekas and R. D. McIntosh, *Organomet. Chem.*, 2021, **43**, 63–82.
- M. Delferro and T. J. Marks, *Chem. Rev.*, 2011, **111**, 2450–2485.
- C. Redshaw, M. J. Walton, D. S. Lee, C. Jiang, M. R. J. Elsegood and K. Michiue, *Chem. – Eur. J.*, 2015, **21**, 5199–5210.
- (a) S. Sanz, K. Ferreira, R. D. McIntosh, S. J. Dalgarno and E. K. Brechin, *Chem. Commun.*, 2011, **47**, 9042–9044; (b) T. Kajiwar, R. Shinagawa, T. Ito, N. Kon, N. Iki and S. Miyano, *Bull. Chem. Soc. Jpn.*, 2003, **76**, 2267–2275.
- A. W. Addison, T. N. Rao, J. Reedijk, J. van Rijn and G. C. Verschoor, *J. Chem. Soc., Dalton Trans.*, 1984, 1349–1356.
- A. L. Spek, *Acta Crystallogr.*, 1990, **A46**, C34.
- G. Wilkinson, G. B. Young, M. Bochmann, M. B. Hursthouse and K. M. A. Malik, *J. Chem. Soc., Dalton Trans.*, 1980, 1863–1871.
- C. Redshaw and M. R. J. Elsegood, *Eur. J. Inorg. Chem.*, 2003, 2071–2074.
- (a) T. Matsuo and H. Kawaguchi, *Inorg. Chem.*, 2002, **41**, 6090–6098; (b) C. Redshaw, M. Rowan, D. M. Homden, M. R. J. Elsegood, T. Yamato and C. Pérez-Casas, *Chem. – Eur. J.*, 2007, **13**, 10129–10139.
- M. H. Chisholm, K. Folting, J. C. Huffman and E. M. Kober, *Inorg. Chem.*, 1985, **24**, 241–245.

